Cooling and trapping of atoms and molecules by counterpropagating pulse trains

V. I. Romanenko,[1,*] Ye. G. Udovitskaya,[1] A. V. Romanenko,[2] and L. P. Yatsenko[1]
[1]*Institute of Physics, National Academy of Sciences of Ukraine, 46 Nauky Avenue, Kyiv 03650, Ukraine*
[2]*Taras Shevchenko National University of Kyiv, 2 Academician Glushkov Avenue, Kyiv 03022, Ukraine*
(Received 24 August 2014; published 19 November 2014)

We discuss a possible one-dimensional trapping and cooling of atoms and molecules due to their nonresonant interaction with counterpropagating light pulse trains. The counterpropagating pulses form a one-dimensional trap for atoms and molecules and a properly chosen carrier frequency detuning from the transition frequency of the atoms or molecules keeps the temperature of the atomic or molecular ensemble close to the Doppler cooling limit. The calculation by the Monte Carlo wave-function method is carried out for the two-level and three-level schemes of the atom's and the molecule's interaction with the field, respectively. The models discussed are applicable to atoms and molecules with almost diagonal Frank-Condon factor arrays. Illustrative calculations are carried out for ensemble-averaged characteristics for sodium atoms and SrF molecules in the trap. The potential for the nanoparticle light pulses's trap formed by counterpropagating light pulse trains is also discussed.

DOI: 10.1103/PhysRevA.90.053421 PACS number(s): 37.10.Gh, 37.10.Mn, 37.10.Pq

I. INTRODUCTION

Optical cooling and trapping [1–3] are key stages in experiments with cold atoms. Initially, continuous laser radiation was used for this purpose, but now pulsed laser applications for cooling [4–11] and trapping [12–16] of atoms and molecules are also discussed. In [4] the deceleration of a Na beam by a counterpropagating beam of a mode-locked laser and the appearance of negative velocity atoms were observed for the first time. The next step to produce cool atoms by pulsed laser radiation was made in [5], where a two-mode laser beam, copropagating with the atomic beam and counterpropagating to the mode-locked laser beam, was used to stop the deceleration process at a defined atomic velocity. In [6] an Yb atomic beam was decelerated with the use of a light beam of a mode-locked Ti:sapphire laser. The first theoretical study of laser cooling of atoms by counterpropagating laser pulses was carried out in [7], where the interaction of atoms with weak laser pulses was analyzed. It was shown that in the case $\gamma \gg \hbar k^2/m$, where γ is the spontaneous emission rate, k is the wave number of laser radiation, m is atomic mass, the atoms' temperature is close to cw case. For a very narrow transition, when $\gamma \ll \hbar k^2/m$, the minimum of the kinetic energy falls behind its cw counterpart. Laser cooling of atoms by an optical frequency comb (FC) was discussed in [8–11]. In particular, laser cooling by the FC on two-photon transitions was proposed in [8]. The theory of light pressure force on two-level and three-level atoms for very short laser pulses (δ-function approximation) and laser cooling was developed in [9–11]. Simultaneous laser cooling of multiple atomic species was discussed in [10].

The authors of [12] showed that the force resulting from the interaction of an atom with a sequence of short counterpropagating laser π pulses can propel atoms towards the small region where the pulses overlap, thus counterpropagating sequences of laser pulses may form an optical trap for atoms. In [13] stimulated focusing and deflection of an atomic Cs beam using counterpropagating picosecond laser pulses were observed that can be treated as experimental justification of the trap idea proposed in [12]. The authors of [14] obtained analytical expressions for the coordinate-dependent force exerted on the atom and the atom's potential energy in the trap based on the trains of counterpropagating laser pulses. References [15,16] consider the semiclassical theory of the atomic dynamics in a pulsed optical dipole trap formed by superimposed trains of very short (a few femtoseconds) laser pulses. The large detuning of the pulse carrier frequency from the transition frequency practically excludes spontaneous emission events. The computer simulation proves that such a trap may effectively confine very cold (∼100 nK) atoms.

Works investigating cooling [4–11] and trapping [12–16] of atoms by sequences of counterpropagating laser pulses are based on the light pressure on atoms. The expected direct consequence of these works is possible simultaneous cooling and trapping of atoms by such laser fields. The authors of [17] analyzed the light pulse interaction with atoms for different detunings and found that simultaneous cooling and trapping of atoms is possible provided the carrier frequency detuning from the resonant atom-light interaction is properly chosen. Further investigation of the cooling trap, based on the interaction of atoms with counterpropagating laser pulses, is described in [18], where numerical calculations for examples of the time evolution of a sodium atom in a trap were demonstrated.

The illustrative simulation of an atom motion in the trap, presented in [17,18], can give only a very rough estimation of the atomic or molecular ensemble temperature and the spatial capture range of the trap. Both these parameters, the temperature and capture range, are main characteristics of any trap. In this paper we find them from the calculation of the statistical characteristics of atomic and molecular ensembles in the trap using the Monte Carlo method. Besides the calculations of the statistical characteristics of the ensembles, we use, as in [17,18], the Monte Carlo wave-function method [19] for simulation of an atom- or a molecule-state evolution. The atomic motion is described in the framework of classical mechanics, which corresponds to a narrow atomic wave packet in comparison with the wavelength. The light pressure force

*vr@iop.kiev.ua

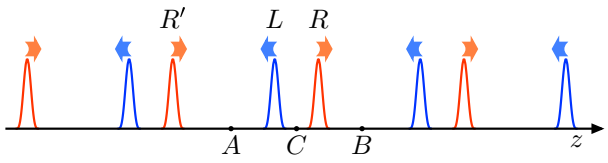

FIG. 1. (Color online) Counterpropagating laser pulses form a trap for atoms near point C, where the pulses collide.

on the atom or the molecule is calculated in the usual way [20,21]. The atomic or molecular momentum is also changed due to spontaneous emission, which is a stochastic process. In comparison to earlier works [17,18], here we take into account the stochastic nature of absorption, proceeding from the fact that every spontaneous emission of a photon precedes the act of a photon absorption. This approach gives rise to the twofold correction of the ensemble temperature in comparison with the method used in [17,18].

The idea of the trap based on the atom's interaction with the counterpropagating light pulse trains can be most easy explained for the case of two-level atoms in the field of π pulses. We let light pulses propagate along the z axis (see Fig. 1) and point C is the point where the counterpropagating pulses collide. We assume that an atom at point A is in the ground state before the recent interaction with pulse R (this is true in most cases because of the short time between the interaction of the atom with R and L pulses in comparison with the time between the interaction with R and R' pulses [22]). As a result of the interaction with this pulse, the atom absorbs a photon and becomes excited. Its momentum is changed by the photon momentum $\hbar k$ in the positive-z-axis direction. After being subjected to the action of pulse L, the atom emits a photon, becomes unexcited, and its momentum changes by another $\hbar k$ in the same direction. The interaction of the atom with the laser pulses repeats with period T, so the atom is subjected to the action of the average force $2\hbar k/T$ directed towards point C. Similar reasoning for an atom at point B allow us to find that the atomic momentum changes by $-2\hbar k$, so the average force acting on it is $-2\hbar k/T$, i.e., directed towards point C. From symmetry considerations we readily conclude that the light pressure force on the atom at point C equals zero. Hence, counterpropagating light π pulses can form a trap for an atom with the center at point C, where the counterpropagating pulses collide. As pointed out in [12,13], pulses with areas different from π can also form a trap.

Recently, great progress in the manipulation of molecules by laser radiation was reported [23]. The authors of [23] demonstrated deceleration of a beam of neutral strontium monofluoride molecules using radiative forces. The spectroscopic constants of this molecule satisfy the main conditions required for successful laser cooling, which are [24] (i) a band system with strong one-photon transitions (i.e., large oscillator strength) to ensure the high photon-scattering rates needed for rapid laser cooling, (ii) a highly diagonal Franck-Condon array for the band system, and (iii) no intervening electronic states to which the upper state could radiate and terminate the cycling transition. We note that violation of the second criterion leads to very high (about 97%) losses of the ground working state of Na_2 in the first observation of the light pressure force on molecules [25].

We illustrate the phenomenon of simultaneous cooling and trapping of atoms and molecules by counterpropagating light pulse trains using examples of sodium atoms and strontium monofluoride molecules, which have a level structure suitable for light pressure force experiments [20,23]. We use the two-level model for an atom, as it adequately describes the cycling cooling transition [20], and the three-level Λ model for a molecule, as 0.9996 of the excited molecules radiatively decay to the two lower levels [23]. The potential for trapping of nanoparticles is briefly discussed in Sec. VII C.

This paper is organized as follows. In Sec. II we present the models for atoms and molecules used in the paper. Section III describes the trains of the counterpropagating pulses that act on the atoms and the molecules. The solution of the Schrödinger equation by the Monte Carlo wave-function method is described in Sec. IV, closely following [19]. Section V contains the calculation of light pressure force and equations for mechanical motion of atoms and molecules. In Sec. VI we describe the numerical calculation routine used in the investigation. Results and a discussion are presented in Sec. VII. A summary is given in Sec. VIII.

II. MODELS FOR ATOMS AND MOLECULES

We use the two-level model for the description of the atom-field interaction. The transitions in atoms, which ensure the cycling interaction with the field within the two-level system, are listed, for example, in [20]. We denote the ground state by g and the excited state by e [see Fig. 2(a)]. The detuning of the carrier frequency ω from the transition frequency ω_0 is $\delta = \omega_0 - \omega$ and the rate of the atom's spontaneous emission from the excited state is γ.

We describe the molecule's interaction with the field by the three-level Λ model, as depicted in Fig. 2(b). This model is composed of the excited state e and the ground states g_1 and g_2 separated by $\hbar\Delta$. The transition frequencies between the excited state and each of the ground states are ϖ_1 and ϖ_2, respectively. These frequencies differ for the SrF molecule, whose interaction with the laser pulses is simulated in this paper, by $\Delta/2\pi = 14.9$ THz [23]. As long as $2\pi/\Delta$ is very small in comparison with the pulse duration τ, we need two pairs of pulse trains, one of which is the counterpropagating pulses close to the resonance with the $e \leftrightarrow g_1$ transition and the other is the counterpropagating pulses close to the resonance with the $e \leftrightarrow g_2$ transition. The carrier frequencies of these pulses ω_1 and ω_2 are detuned from the resonances by $\delta_1 = \varpi_1 - \omega_1$ and $\delta_2 = \varpi_2 - \omega_2$, respectively. We also introduce the spontaneous decay rates γ_1 and γ_2 from the upper state to the two lower states, which form the total decay rate $\gamma = \gamma_1 + \gamma_2$.

III. LASER PULSES

We suppose that the pairs of pulses traveling in the same direction (and resonant to the different transitions) coincide in time. The spectrum of the laser field is a frequency comb with the difference between the teeth $2\pi/T$, where T is the repetition period of the laser pulses.

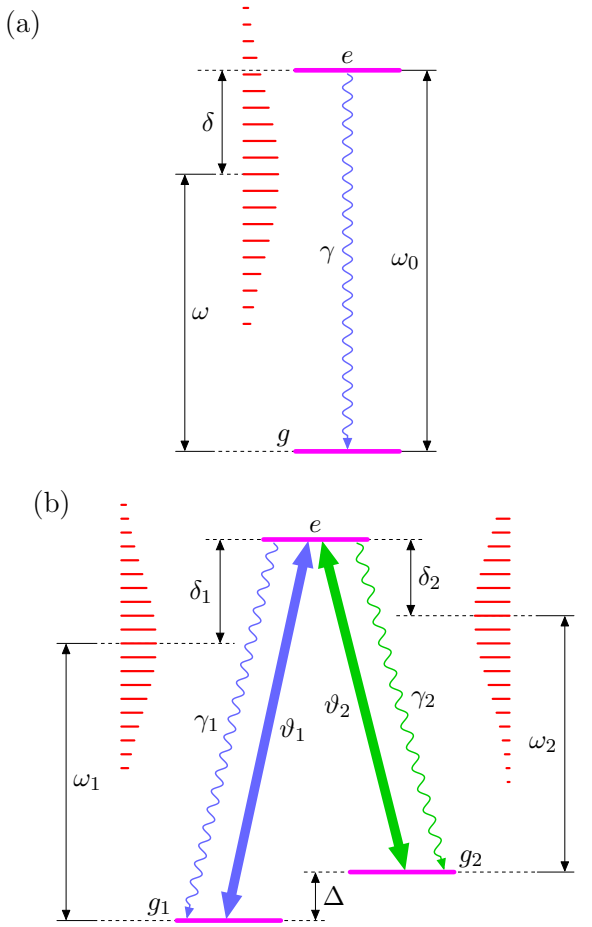

FIG. 2. (Color online) (a) Two-level scheme of the atom-field interaction and (b) three-level scheme of the molecule interaction with the field of laser radiation.

The electric field of the trains of the counterpropagating pulses can be written as

$$\begin{aligned}\mathbf{E}(t) = {} & E_1\mathbf{e}_1\sum_m \cos(\omega_1 t - k_1 z + \varphi_{11,m}) f(\eta_{1,m}) \\ & + E_1\mathbf{e}_1\sum_m \cos(\omega_1 t + k_1 z + \varphi_{12,m}) f(\eta_{2,m}) \\ & + E_2\mathbf{e}_2\sum_m \cos(\omega_2 t - k_2 z + \varphi_{21,m}) f(\eta_{1,m}) \\ & + E_2\mathbf{e}_2\sum_m \cos(\omega_2 t + k_2 z + \varphi_{22,m}) f(\eta_{2,m}). \quad (1)\end{aligned}$$

Here $k_1 = \omega_1/c$ and $k_2 = \omega_2/c$ are the values of the wave vectors for carrier frequencies ω_1 and ω_2, respectively; $\mathbf{e}_1$ and $\mathbf{e}_2$ are polarization vectors; and $\varphi_{11,m}$,$\varphi_{12,m}$ and $\varphi_{21,m}$,$\varphi_{22,m}$ are the phases of the counterpropagating m pulses for $t = 0$ and $z = 0$, respectively. The function $f(\eta)$ with a maximum value $f(0) = 1$ describes the shape of the pulse's envelope,

$$\eta_{1,m} = \frac{1}{\tau}\left(t - mT - \frac{z}{c}\right), \quad (2)$$

$$\eta_{2,m} = \frac{1}{\tau}\left(t - mT + \frac{z}{c}\right), \quad (3)$$

where z is the atom's or molecule's coordinate and τ is the pulse duration. The beginning of the coordinate axis and the order of the pulses numbering are chosen so that the counterpropagating pulses' number m meet each other at time instants $t = mT$ in point $z = 0$, where m is an arbitrary integer.

The pulse areas are defined by the integrals

$$\vartheta_j = \Omega_j \int_{-\infty}^{\infty} f(t/\tau)dt, \quad j = 1,2, \quad (4)$$

where the Rabi frequencies are

$$\Omega_j = -\mathbf{d}_{g_j e}\mathbf{e}_j E_j/\hbar, \quad j = 1,2. \quad (5)$$

The matrix elements $\mathbf{d}_{g_j e} = \langle g_j|\mathbf{d}|e\rangle$ of the dipole moments are assumed to be the real-value quantities without loss of generality [26]. The case of the two-level model [Fig. 2(a)] is described by the equations of this section with $\gamma_1 = \gamma$, $\gamma_2 = 0$, $\vartheta_1 = \vartheta$, $\vartheta_2 = 0$, $\omega_1 = \omega$, $\delta_1 = \delta$, and $\varpi_1 = \omega_0$.

Usually the Gaussian-like pulses are used in simulations of the atom-field interactions [27,28]. These pulses are artificially cut off beyond certain limits in the numerical calculation. We use $\cos^4$-like pulses that are close to Gaussian but restricted in time as real laser pulses,

$$f(\eta) = \begin{cases}\cos^4(\pi\eta), & |\eta| < 1/2 \\ 0, & |\eta| > 1/2.\end{cases} \quad (6)$$

The function $f(\eta)$ is close to the Gaussian distribution $f_G(\eta) = \exp(-2\pi^2\eta^2)$ in the interval where $f_G(\eta)$ is not very small. The area of the pulse with the envelope described by the function (6) equals $\frac{3}{8}\Omega_0\tau$, which is approximately 0.94 times the area of the corresponding Gaussian pulse. The characteristic width of the latter is $\tau_G \approx 0.225\tau$. A closer adjustment of the $\cos^n$-like pulse to the Gaussian pulse is possible: The function $\cos^n(\pi t/\tau)$ tends to $\exp(-t^2/\tau_G^2)$ with $\tau_G = \tau\sqrt{2}(\pi\sqrt{n})^{-1}$ for large even n within the interval $|t| < \tau/2$ [29].

IV. WAVE-FUNCTION CALCULATION

We describe the atomic state by the wave function that is constructed by the Monte Carlo wave-function (MCWF) method [19]. After averaging over the ensemble of atoms or molecules, this approach becomes equivalent to the solution of the density-matrix equation. At the same time, in contrast to the latter, it allows one to give an illustrative interpretation for the separate atom's or molecule's motion.

The wave function obeys the Schrödinger equation

$$i\hbar\frac{d}{dt}|\psi\rangle = H|\psi\rangle, \quad (7)$$

where the Hamiltonian

$$\begin{aligned}H = {} & \hbar\varpi_1|e\rangle\langle e| + \hbar\Delta|g_2\rangle\langle g_2| - \mathbf{d}_{g_1 e}|g_1\rangle\langle e|\mathbf{E}(t) \\ & - \mathbf{d}_{eg_1}|e\rangle\langle g_1|\mathbf{E}(t) - \mathbf{d}_{g_2 e}|g_2\rangle\langle e|\mathbf{E}(t) \\ & - \mathbf{d}_{eg_2}|e\rangle\langle g_2|\mathbf{E}(t) - \frac{i\hbar}{2}(\gamma_1 + \gamma_2)|e\rangle\langle e|, \quad (8)\end{aligned}$$

which is used for the construction of the wave function by the MCWF method, differs in the relaxation term from the Hamiltonian that is used in the density-matrix equation. The Hamiltonian (8) is non-Hermitian, hence the absolute value of the wave function determined from the Schrödinger equation (7) changes with time. In the MCWF method, normalization of the wave function should be carried out after every small time step. In addition, the condition of a quantum jump within each time interval has to be checked [19].

We use the first-order method for calculation of the Monte Carlo wave function [19]. The second- and the fourth-order methods are described in [30].

We let the wave function $|\psi(t)\rangle$ be normalized to unity at the time moment t. After a small time step Δt the wave function $|\psi(t)\rangle$ is transformed into

$$|\psi^{(1)}(t+\Delta t)\rangle = \left(1 - \frac{i\Delta t}{\hbar} H\right)|\psi(t)\rangle \tag{9}$$

according to the Schrödinger equation (7). The squared norm of the wave function equals

$$\langle\psi^{(1)}(t+\Delta t)|\psi^{(1)}(t+\Delta t)\rangle = 1 - \Delta P, \tag{10}$$

where

$$\begin{aligned}\Delta P &= \frac{i\Delta t}{\hbar}\langle\psi(t)|H - H^{\dagger}|\psi(t)\rangle \\ &= (\gamma_1+\gamma_2)\langle\psi(t)|e\rangle\langle e|\psi(t)\rangle\Delta t.\end{aligned} \tag{11}$$

Now we take into account the possibility of a quantum jump. If the value of the random variable ϵ, which is uniformly distributed between zero and unity, is larger than ΔP (which is true in the most cases, as long as $\Delta P \ll 1$), there is no jump. Then the wave function at the time moment $t+\Delta t$ equals

$$|\psi(t+\Delta t)\rangle = |\psi^{(1)}(t+\Delta t)\rangle/\sqrt{1-\Delta P}, \quad \Delta P < \epsilon. \tag{12}$$

In the opposite case $\epsilon < \Delta P$, the jump occurs and the wave functions becomes

$$|\psi(t+\Delta t)\rangle = |g_1\rangle \tag{13}$$

with probability $p_1 = \gamma_1/(\gamma_1+\gamma_2)$ or

$$|\psi(t+\Delta t)\rangle = |g_2\rangle \tag{14}$$

with probability $p_2 = \gamma_2/(\gamma_1+\gamma_2)$. If the value of the random variable ϵ, uniformly distributed between 0 and 1, is less than p_1, the wave function is (13); otherwise it is (14).

It is convenient to separate the rapid component, varying with the frequency ϖ_1, in the wave function. For this purpose we seek the solution of (7) in the form

$$|\psi\rangle = C_{g_1}|g_1\rangle + C_2 e^{-i\Delta t}|g_2\rangle + C_e e^{-i\varpi_1 t}|e\rangle. \tag{15}$$

After applying the rotating-wave approximation [26] to the Schrödinger equation we find, assuming $\Delta \ll \varpi_1$, the equations for probability amplitudes

$$\begin{aligned}\frac{d}{dt}C_{g_1} &= -\frac{i}{2}\Omega_1 e^{-ikz-i\delta_1 t}\sum_m e^{i\varphi_{11,m}} f(\eta_{1,m})C_e \\ &\quad -\frac{i}{2}\Omega_1 e^{ikz-i\delta_1 t}\sum_m e^{i\varphi_{12,m}} f(\eta_{2,m})C_e,\end{aligned} \tag{16}$$

$$\begin{aligned}\frac{d}{dt}C_{g_2} &= -\frac{i}{2}\Omega_2 e^{-ikz-i\delta_2 t}\sum_m e^{i\varphi_{21,m}} f(\eta_{1,m})C_e \\ &\quad -\frac{i}{2}\Omega_2 e^{ikz-i\delta_2 t}\sum_m e^{i\varphi_{22,m}} f(\eta_{2,m})C_e,\end{aligned} \tag{17}$$

$$\begin{aligned}\frac{d}{dt}C_e &= -\frac{i}{2}\Omega_1 e^{ikz+i\delta_1 t}\sum_m e^{-i\varphi_{11,m}} f(\eta_{1,m})C_{g_1} \\ &\quad -\frac{i}{2}\Omega_1 e^{-ikz+i\delta_1 t}\sum_m e^{-i\varphi_{12,m}} f(\eta_{2,m})C_{g_1} \\ &\quad -\frac{i}{2}\Omega_2 e^{ikz+i\delta_2 t}\sum_m e^{-i\varphi_{21,m}} f(\eta_{1,m})C_{g_2} \\ &\quad -\frac{i}{2}\Omega_2 e^{-ikz+i\delta_2 t}\sum_m e^{-i\varphi_{22,m}} f(\eta_{2,m})C_{g_2} - \frac{\gamma_1+\gamma_2}{2}C_e,\end{aligned} \tag{18}$$

which are to be numerically solved simultaneously with the quantum jump testing.

Most of the time (during the time interval between the light pulses) the field does not influence the atom or the molecule. In this case an analytical solution of Eqs. (16)–(18) is possible. The initial atom or molecule state is

$$|\psi(0)\rangle = C_{g_1}(0)|g_1\rangle + C_{g_2}(0)|g_2\rangle + C_e(0)|e\rangle. \tag{19}$$

If no quantum jump occurs within the time interval $[0,t]$, we find from Eqs. (16)–(18) the normalized wave function

$$\begin{aligned}|\psi(t)\rangle &= C_{g_1}(t)|g_1\rangle + C_{g_2}(t)e^{-i\Delta t}|g_2\rangle \\ &\quad + C_e(t)e^{-i\varpi_1 t}|e\rangle,\end{aligned} \tag{20}$$

where

$$C_{g_1}(t) = C_{g_1}(0)/D, \tag{21}$$

$$C_{g_2}(t) = C_{g_2}(0)/D, \tag{22}$$

$$C_e(t) = C_e(0)e^{-(\gamma_1+\gamma_2)t/2}/D, \tag{23}$$

and

$$D = \sqrt{|C_{g_1}(0)|^2 + |C_{g_2}(0)|^2 + |C_e(0)|^2 e^{-(\gamma_1+\gamma_2)t}}. \tag{24}$$

The probability of the absence of a quantum jump within the time interval $[0,t]$ is [19]

$$P(t) = |C_1(0)|^2 + |C_2(0)|^2 + |C_e(0)|^2 e^{-(\gamma_1+\gamma_2)t}. \tag{25}$$

The expression (25) is consistent with the probability $|C_1(0)|^2 + |C_2(0)|^2$ of no quantum jump for $t \to \infty$ and the exponential decay of the excited state in the ensemble of atoms or molecules.

So, in summary, in the absence of laser radiation within the time interval $[0,t]$, the atom or molecule is described by the state (20) at the time instant t with the probability (25). The other possible states are

$$|\psi(t)\rangle = |g_1\rangle \tag{26}$$

with the probability $\gamma_1[1-P(t)]/(\gamma_1+\gamma_2)$ and

$$|\psi(t)\rangle = |g_2\rangle \tag{27}$$

with the probability $\gamma_2[1-P(t)]/(\gamma_1+\gamma_2)$.

V. MOTION OF THE ATOM AND THE MOLECULE

Cooling of atoms in one-dimensional molasses was successfully simulated by the MCWF method in [19]. In this case only the atomic momentum distribution function matters. Analyzing possible simultaneous cooling and trapping of atoms or molecules in the considered trap, we need both the spatial and momentum distribution functions. Quantum-mechanical calculation of the atomic motion in the trap should start from the wave package with spatial width much less than the laser radiation wavelength. As a consequence, many momentum states of the atom in both the ground and excited states are involved in the calculation.

The computation time can be substantially reduced for the case of weak laser fields, when the momentum diffusion of the atoms could be treated as caused by counterpropagating laser pulses independently. In this case we consider the atom's motion in the framework of classical mechanics and we need to know the light pressure force that the atoms undergo. This force can be calculated from the density matrix and the electric field of the pulses [20,21],

$$F = \sum_{j=1}^{2} (\varrho_{g_j e}\mathbf{d}_{eg_j} + \varrho_{eg_j}\mathbf{d}_{g_j e})\frac{\partial \mathbf{E}}{\partial z}, \tag{28}$$

where the density-matrix elements are expressed in terms of C_{g_1}, C_{g_2}, and C_e as follows:

$$\varrho_{g_j g_j} = |C_j|^2, \quad j = 1,2, \tag{29}$$

$$\varrho_{ee} = |C_e|^2, \tag{30}$$

$$\varrho_{eg_1} = C_1^* C_e e^{-i\varpi_1 t}, \tag{31}$$

$$\varrho_{g_1 e} = C_1 C_e^* e^{i\varpi_1 t}, \tag{32}$$

$$\varrho_{eg_2} = C_2^* C_e e^{-i\varpi_2 t}, \tag{33}$$

$$\varrho_{g_2 e} = C_2 C_e^* e^{i\varpi_2 t}. \tag{34}$$

We assume that the pulse duration considerably exceeds the inverse carrier frequencies $\omega_1\tau \gg 1$ and $\omega_2\tau \gg 1$, therefore we neglect the derivative of the pulse's envelope in the calculation of the time derivative of the field strength, as long as $|\frac{\partial f(\eta_{j,m})}{\partial z}| \ll k_j f(\eta_{j,m})$ $(j = 1,2)$.

After averaging over the period of oscillations with the frequency ω_1, the expression (28) in the field (1) gives

$$\begin{aligned} F = \Bigg[& \hbar k_1 \Omega_1 \,\mathrm{Im}\, C_1 C_e^* e^{i\delta_1 t + ik_1 z} \sum_m e^{-i\varphi_{11,m}} f(\eta_{1,m}) \\ & + \hbar k_2 \Omega_2 \,\mathrm{Im}\, C_2 C_e^* e^{i\delta_2 t + ik_2 z} \sum_m e^{-i\varphi_{21,m}} f(\eta_{1,m}) \\ & - \hbar k_1 \Omega_1 \,\mathrm{Im}\, C_1 C_e^* e^{i\delta_1 t - ik_1 z} \sum_m e^{-i\varphi_{12,m}} f(\eta_{2,m}) \\ & - \hbar k_2 \Omega_2 \,\mathrm{Im}\, C_2 C_e^* e^{i\delta_2 t - ik_2 z} \sum_m e^{-i\varphi_{22,m}} f(\eta_{2,m}) \Bigg] \\ & \times [|C_1|^2 + |C_2|^2 + |C_e|^2]^{-1}. \end{aligned} \tag{35}$$

We find the dependence of the atom's coordinate z on time from Newton's equation

$$\ddot{z} = F/M, \tag{36}$$

where M is the atom's mass. We consider the case $|\varpi_1 - \varpi_2| \ll \varpi_1$ and assume that $k_1 = k_2$ in (35).

Equation (36) does not take into account the momentum change due to spontaneous emission of photons. Every event of spontaneous emission of a photon change the atom's or the molecule's velocity by $\hbar\boldsymbol{k}/M$ in the random direction with the probability $1 - P(t)$, where P is determined by (25). In addition, the velocity also changes due to fluctuations of absorption and stimulated emission of photons.

VI. NUMERICAL CALCULATION ROUTINE

To simulate the atom's or molecule's motion, we simultaneously solve Eqs. (16)–(18) and (36), where the light pressure force we find from (35). In addition, we take into account both the atomic momentum's change due to the spontaneous emission of photons and fluctuation of stimulated (absorption and emission) processes. In our model calculations we postulate that spontaneous emission occurs with equal probability in two directions along the light beam, so the atom's or molecule's momentum changes by $\pm\hbar k$. This assumption in analyses of Doppler cooling leads to the minimum temperature [31]

$$T_{\min} = \hbar\gamma/2k_B, \tag{37}$$

where k_B is the Boltzmann constant and γ is the rate of the spontaneous emission of radiation by the excited atom.

The expression (28) for the light pressure force gives the correct value for the ensemble-average force, but the momentum diffusion phenomenon is not correctly taken into account. To analyze the motion of atoms or molecules in the trap we need to add the stochastic change of the momentum, zero on average, which gives the correct momentum diffusion coefficient. We analyze the low-intensity case, when the population of the excited state is small and the light pressure force and the momentum diffusion approximately equal the sum of the corresponding values for each of the counterpropagating traveling waves. Here we describe the momentum diffusion of atoms in the field of one traveling wave following [21].

We let the momentum of an atom at the time instant t be $\mathbf{p}_0$. Then at the time instant $t + \Delta t$ the momentum is

$$\mathbf{p} = \mathbf{p}_0 + \hbar\mathbf{k}(N_+ - N_-) - \sum_s \hbar\mathbf{k}_s. \tag{38}$$

Here the second term gives the change of momentum due to absorption and stimulated emission, when the photons with the wave vector $\mathbf{k}$ (directed along the z axis) are absorbed and emitted. The quantities N_+ and N_- are the numbers of absorbed and emitted photons. The third term in (38) is responsible for the momentum change due to the spontaneous emission of the photons with the wave vector $\mathbf{k}_s$.

The ensemble average of the momentum (38) is

$$\langle\mathbf{p}\rangle = \langle\mathbf{p}_0\rangle + \hbar\mathbf{k}(\langle N_+\rangle - \langle N_-\rangle), \tag{39}$$

where $\langle\mathbf{p}_0\rangle$ is the initial average momentum, $\langle N_+\rangle$ is the average number of absorbed photons, and $\langle N_-\rangle$ is the average

number of photons emitted by atoms in the process of stimulated emission. The photons emitted in the process of spontaneous emission do not change the average momentum

$$\left\langle \sum_s \mathbf{k}_s \right\rangle = 0. \quad (40)$$

The difference between (38) and (39) gives the momentum fluctuation

$$\Delta\mathbf{p} = \mathbf{p} - \langle\mathbf{p}\rangle = (\mathbf{p}_0 - \langle\mathbf{p}_0\rangle) + \hbar\mathbf{k}\Delta N_i - \sum_s \hbar\mathbf{k}_s, \quad (41)$$

where $\Delta N_i = N_i - \langle N_i\rangle$ is the variation of the difference $N_i = N_+ - N_-$ from the corresponding ensemble-average value.

The average square of the momentum fluctuations along the z axis is

$$\langle\Delta p_z^2\rangle = \langle\Delta p_{0z}^2\rangle + \hbar^2k^2\langle(\Delta N_i)^2\rangle + \hbar^2k^2\langle\cos^2\theta\rangle\langle N_s\rangle. \quad (42)$$

Here θ is the angle between the direction of the photon's spontaneous emission and the z axis and $\langle N_s\rangle$ is the average number of spontaneously emitted photons. The first term on the right-hand side of (42) gives the initial momentum spreading, the second term is due to stimulated processes (absorption and emission), and the third term is due to spontaneous emission.

Let us find $\langle(\Delta N_i)^2\rangle$ by assuming the Poisson photons statistics. In this case

$$\langle(\Delta N_i)^2\rangle = \langle N_i\rangle. \quad (43)$$

Noting that $\langle N_i\rangle = \langle N_s\rangle$, we finally find

$$\langle\Delta p_z^2\rangle = \langle\Delta p_{0z}^2\rangle + \hbar^2k^2\langle N_s\rangle + \hbar^2k^2\langle\cos^2\theta\rangle\langle N_s\rangle. \quad (44)$$

This equation shows the way for numerical modeling of the momentum diffusion process in the field of a traveling wave. Each random momentum change due to spontaneous emission is accompanied by the stimulated process, in which the momentum of the atom is changed by $\pm\hbar k$.

Now we consider the case of counterpropagating laser pulses. When counterpropagating laser pulses are weak, spontaneous emission follows each absorbed photon, so the fluctuation events of the atomic or molecular velocity change due to light-induced processes occur as frequently as events of spontaneous emission. This point is the background of our computer simulation of atom and molecule movement in the field of laser radiation.

In our calculation we assume the model of $\pm\hbar k$ change of momentum due to spontaneous emission (θ equals 0 or π with equal probability). We use different approaches to solving Eqs. (16)–(18), (36), and (35) during the atom's interaction with the pulses and free evolution of the atom. In the first case the solution to this set of equations is found by using the Runge-Kutta fourth-order method with a fixed step size. After every step we check if a quantum jump occurs and normalize the wave function. If a jump occurs, the atom's velocity changes by

$$\Delta v = \hbar k(\epsilon_1 - 0.5)|/(M|\epsilon_1 - 0.5|) + \hbar k(\epsilon_2 - 0.5)|/(M|\epsilon_2 - 0.5|),$$

where $\epsilon_{1,2}$ are random numbers with a uniform distribution in the interval $[0,1]$. In the second case, when the field does not act on the atom, we do not need to divide the considered time interval by small subintervals and check if the quantum jump occurs in every subinterval. Knowing the probability (25) of the absence of a quantum jump within the time interval $[0,t]$, we simulate the time moment of the quantum jump. The scheme of calculation is the following. We compare the value of the random variable ϵ uniformly distributed in the interval $[0,1]$ with $|C_1(0)|^2 + |C_2(0)|^2$ at the beginning of the time interval. A jump occurs if $\epsilon > |C_1(0)|^2 + |C_2(0)|^2$ and does not otherwise. In the latter case the wave function is described by Eqs. (15) and (21)–(23). If a jump occurs, we simulate the time moment of the quantum jump. We take a random ϵ, which is uniformly distributed in the interval $[0,1]$. For the exponential distribution of probability $P_e = e^{-(\gamma_1+\gamma_2)t}$, the quantity $t_{\text{jump}} = -(\ln\epsilon)(\gamma_1+\gamma_2)^{-1}$ simulates the time moment when the jump occurs [32]. If t_{jump} exceeds the time interval between the laser pulses, we calculate the probability amplitudes (21)–(23) at the beginning of the next pulse; otherwise we calculate the atom's velocity change

$$\Delta v = \hbar k(\epsilon_1 - 0.5)|/(M|\epsilon_1 - 0.5|) + \hbar k(\epsilon_2 - 0.5)|/(M|\epsilon_2 - 0.5|)$$

at t_{jump} using random numbers $\epsilon_{1,2}$ with a uniform distribution in the interval $[0,1]$. The atom's or molecule's state is (26), with the probability $\gamma_1[1 - P(t)]/(\gamma_1+\gamma_2)$, or (27), with the probability $\gamma_2[1 - P(t)]/(\gamma_1+\gamma_2)$. To choose between these states, we compare $\gamma_1/(\gamma_1+\gamma_2)$ with a new random value ϵ. When $\epsilon < \gamma_1/(\gamma_1+\gamma_2)$, the state of the atom or the molecule is described by (26); otherwise it is described by the wave function (27).

The described approach substantially reduces the calculation time in comparison with the Runge-Kutta method during the whole time of the atom's or the molecule's motion. To estimate the temperature of the captured atoms or molecules, we average the velocity and the squared velocity over the ensemble of particles.

VII. RESULTS AND DISCUSSION

In this section we describe the results of the numerical simulation of the atoms' and molecules' motion in the trap formed by the trains of counterpropagating light pulses. In contrast to the results of [17,18], where the evolution of two-level atoms was investigated, here we also study statistical characteristics of the atomic and molecular ensembles.

We analyze the simplest models of the atom-field and the molecule-field interaction. It is well known that the cycling atom-field interaction can be realized between two states of some atoms [20]. As an example of such an interaction, we chose the $3\,^2S_{1/2}$–$3\,^2P_{3/2}$ transition in the sodium atom. The simplest molecule-field interaction model include three levels. The transitions coupling the state $A\,^2\Pi_{1/2}(v' = 0, J' = 1/2)$ with the states $X\,^2\Sigma^+_{1/2}(v = 0, N = 1)$ and $X\,^2\Sigma^+_{1/2}(v = 1, N = 1)$ of SrF form the almost close three-level Λ scheme [23]. The spontaneous emission from the upper state leads the molecule to the lower states with the probability 0.9996. Including the state $X\,^2\Sigma^+_{1/2}(v = 2, N = 1)$ in the considered model gives a probability of the spontaneous transition to the three lower states more than 0.9999, but we do not add this state, possibly sacrificing the simulation accuracy for the sake

of greater physical clarity. Anyway, an additional light field can return the molecules that are lost from the scheme due to spontaneous emission, as realized in experiment [23].

A. Two-level model

The investigation of simultaneous trapping and cooling of atoms by the counterpropagating laser pulses is presented in Refs. [17,18] for the two-level model of the atom-field interaction. In [17] the momentum diffusion of the two-level atoms in an optical trap formed by sequences of counterpropagating light pulse trains was studied and it was discovered that proper detuning of the carrier frequency of laser pulses from the resonance with the atom's transition frequency leads to cooling of the atomic ensemble. The other sign of detuning, as well as the resonant interaction of the field with atoms, leads to heating of the atomic ensemble. The conclusions of [17] are based on the computer simulation of the motion of an atom in the trap for hypothetical atomic and atom-field interaction parameters. In [18] the motion of the ^{23}Na atom in the trap was analyzed. Here we take the next step in the pulse trap investigation, which includes the simulation of the atomic ensemble characteristics.

The possible cooling of atoms in the trap can be easily explained for weak pulses $\vartheta \ll \gamma T$, where $\vartheta \equiv \vartheta_1$ is the pulse area $\gamma \equiv \gamma_1$. In this case the atom mostly interacts with the spectral component of the pulses trains that is closest to the transition frequency. We let the carrier frequency of the pulses be tuned below the transition frequency in the atom. Then the atoms, due to the Doppler effect, always absorb more photons from the laser beam opposite to their direction of motion. As a result, a friction force arises and cools the atoms down to the Doppler cooling limit (37). This limit is caused by the competition between the cooling due to the friction force and heating due to the momentum diffusion. For large pulse areas the detuning of the carrier frequency from the resonance with the transition frequency in the atom, needed for atoms cooling, changes sign [18].

We consider an optical trap that extends from $z = -100$ to 100 mm relative to the point where counterpropagating light pulses collide and trace the motion of an atom until it moves inside the trap. Level g_2 is not taken into account in the simulation of ^{23}Na motion in the trap. In addition, we suppose $\varphi_{11,m} = \varphi_{12,m} = 0$ in (16) and (18). Figure 3 shows an example of the atom's motion in the field of the counterpropagating sequences of 1-ps light pulses with a repetition frequency of 100 MHz. Very quickly (0.14 ms after the beginning of the interaction with the field) the atom slows down to zero velocity and then its velocity fluctuates in the region ± 1 m/s. The atom returns to the center of the trap approximately after 4.7 ms and then fluctuates in the region ± 0.25 mm. The velocity capture range of the trap for the parameters specified in Fig. 3 extends at least from $v = -20$ to 20 m/s (the temperature of the atoms is about 1 K).

To estimate the measure of cooling in the trap, we introduce the temperature of the atomic ensemble by the expression

$$T_a = \frac{m\langle v^2\rangle}{k_B}, \tag{45}$$

where k_B is the Boltzmann constant. The value of T_a coincides with the real temperature of the ensemble in the case of the Maxwell velocity distribution. We expect the cooling process in the trap to be close to the Doppler cooling [20,31], at least for the case of a weak field. This expectation is confirmed by a comparison of the solid curve and the dots in Fig. 4, where the dots were calculated from Eq. (45) with averaging over 1000 sodium atoms and the solid curve represents the dependence of the atoms' temperature on the detuning of the frequency

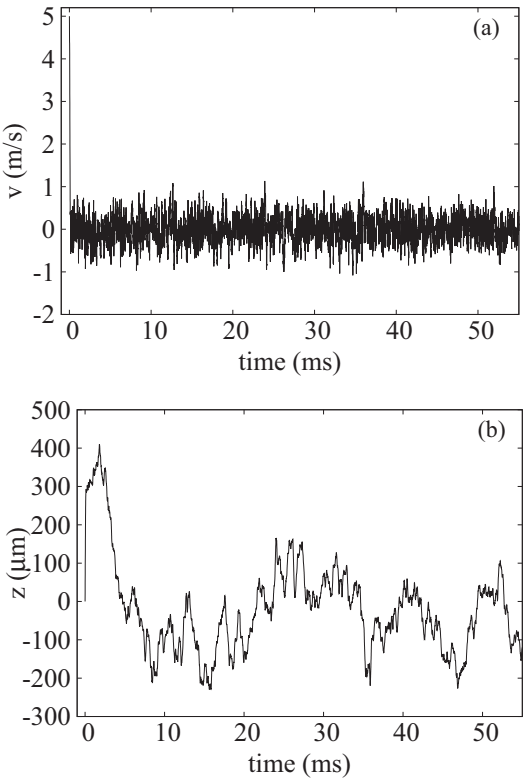

FIG. 3. Example of the sodium atom's motion in the field of the counterpropagating sequences of light pulses: (a) $v(t)$ and (b) $z(t)$. The parameters are $\tau = 1$ ps, $T = 10$ ns, $\vartheta = 0.05\pi$, $\gamma = 2\pi \times 10$ MHz, $\delta = 2\pi \times 5$ MHz, $\lambda = 589$ nm, and $M = 23$ Da. The atom starts at the center of the trap with initial velocity $v_0 = 5$ m/s.

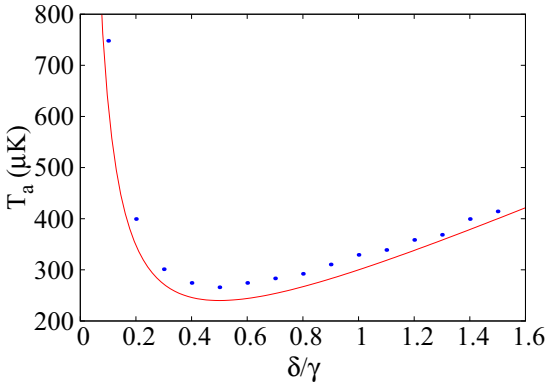

FIG. 4. (Color online) Dependence of the temperature of 1000 sodium atoms in the trap formed by the counterpropagating sequences of light pulses on the pulse's carrier frequency detuning on the atomic transition frequency. The parameters are $\tau = 1$ ps, $T = 10$ ns, $\vartheta = 0.05\pi$, $\gamma = 2\pi \times 10$ MHz, $\lambda = 589$ nm, and $M = 23$ Da.

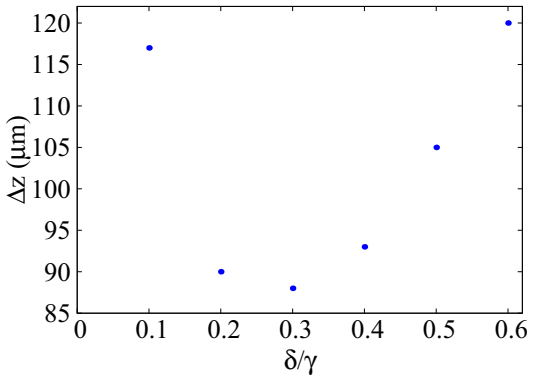

FIG. 5. (Color online) Dependence of the spatial capture range of the trap $\Delta z = \sqrt{\langle z^2\rangle - \langle z\rangle^2}$ on the frequency detuning δ. The parameters are the same as in Fig. 4.

of the weak monochromatic standing wave from the atomic transition frequency [31]

$$T_{\rm SW} = \frac{1}{2} T_{\rm min}\left(\frac{2\delta}{\gamma} + \frac{\gamma}{2\delta}\right). \tag{46}$$

For sodium atoms $T_{\rm min} = 240\ \mu$K [20]. The temperature is minimal, as in the case of the standing wave, for $\delta = \gamma/2$. The difference between the curve and the dots, according to our calculations, becomes smaller for smaller pulse areas.

The spatial capture range of the trap depends on δ and ϑ. The first dependence is depicted in Fig. 5. The value of δ for the minimal capture range does not coincide with δ for the minimal temperature; it is reached at $\delta = 0.3\gamma$. For the parameters used in modeling this dependence, the atoms are localized in the region of the pulses' overlapping. This region becomes narrower when pulse area increases (see Fig. 6).

B. Three-level model

We simulate the dynamics of the three-level system for the parameters that are close to the interaction of SrF with cw laser radiation [23]. Our consideration neglects the probability 0.0004 of the molecule to leave the Λ scheme in the process of spontaneous emission from the excited level (see Fig. 2).

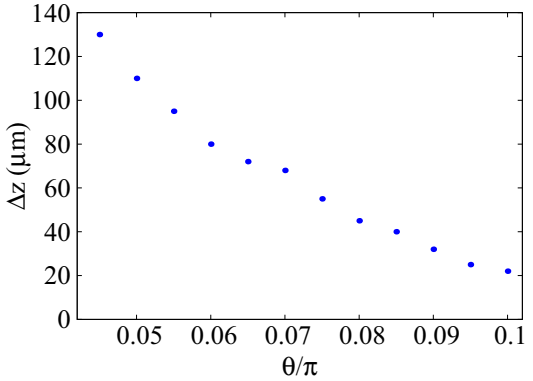

FIG. 6. (Color online) Dependence of the spatial capture range of the trap $\Delta z = \sqrt{\langle z^2\rangle - \langle z\rangle^2}$ on the pulse area for $\delta = 0.5\gamma$. The other parameters are the same as in Fig. 4.

The spontaneous emission rate from the excited state is $\gamma = \gamma_1 + \gamma_2 = 2\pi \times 7$ MHz and the branching ratio $\gamma_2/\gamma_1 = 0.02$. Considering the equal energy of the pulses, we arrive at the conclusion that $\vartheta_2/\vartheta_1 = d_{eg_2}/d_{eg_1} = \sqrt{\gamma_2/\gamma_1} = 0.14$. The wavelengths of the transitions are $\lambda_1 = 663.3$ nm ($e \Leftrightarrow g_1$) and $\lambda_2 = 686.0$ nm ($e \Leftrightarrow g_2$). In the calculation of the photon momentum for each transition we neglect the difference between λ_1 and λ_2. The repetition period of the pulses is chosen to be $T = 23.8$ ns. It corresponds to the period of the frequency modulation of laser radiation in the experiment [23], which provides the excitation of all superfine sublevels of the ground states. The detunings δ_1 and δ_2 should not correspond to the two-photon resonance condition $\delta_2 - \delta_1 = 2\pi n/T$, where n is integer, to avoid the coherent population trapping; otherwise the population of the excited state becomes zero and the light pressure force vanishes [11,33]. As in the case of the two-level model, the pulse duration is $\tau = 1$ ps.

Figure 7 shows an example of the molecule's motion in the field of the counterpropagating sequences of 1-ps light pulses. Very quickly (0.34 ms after the beginning of the interaction with the field) the molecule slows down to zero velocity and then its velocity fluctuates in the region ± 0.4 m/s. The molecule returns to the center of the trap approximately after 5.6 ms and then fluctuates in the region ± 0.25 mm.

Sometimes, in 2% of cases, the excited molecule relax to the g_2 state. As a result, we see in Fig. 7 several almost horizontal

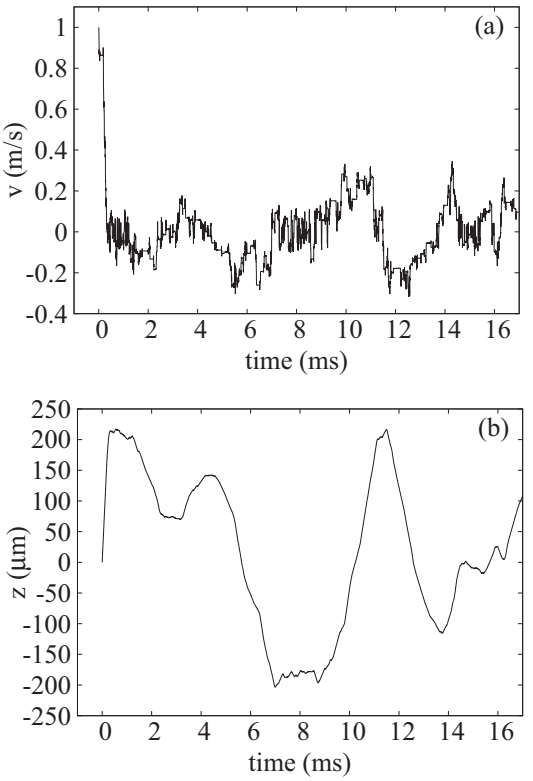

FIG. 7. Example of the SrF molecule motion in the field of the counterpropagating sequences of light pulses: (a) $v(t)$ and (b) $z(t)$. The parameters are $\tau = 1$ ps, $T = 23.8$ ns, $\vartheta_1 = 0.1\pi$, $\vartheta_2 = 0.014\pi$, $\gamma = 2\pi \times 7$ MHz, $\delta_1 = 2\pi \times 3.5$ MHz, $\delta_2 = 2\pi \times 7$ MHz, $\lambda = 663.3$ nm, and $M = 107$ Da. The molecule starts at the center of the trap with initial velocity $v_0 = 1$ m/s.

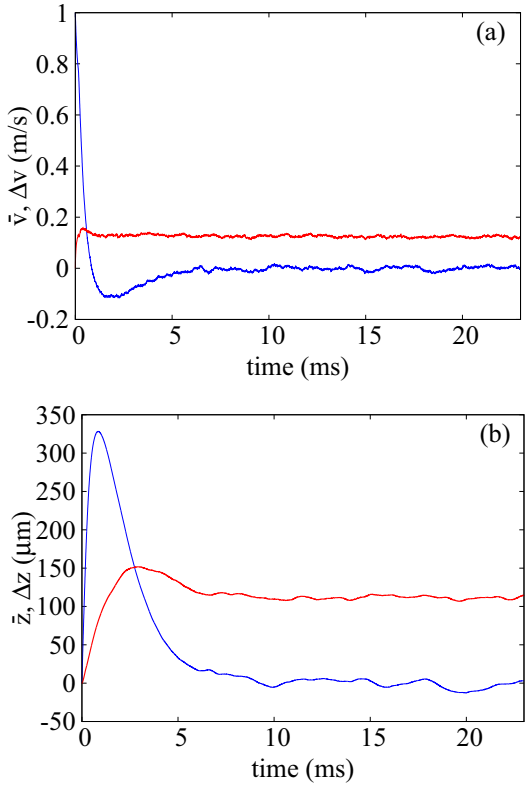

FIG. 8. (Color online) Time dependences of (a) average velocity $\bar{v} = \langle v \rangle$ (thin line) and $\Delta v = \sqrt{\langle v^2 \rangle - \langle v \rangle^2}$ (thick line) and (b) average coordinate $\bar{z} = \langle z \rangle$ (thin line) and Δz (thick line) for an ensemble of 400 molecules. The parameters are the same as in Fig. 7.

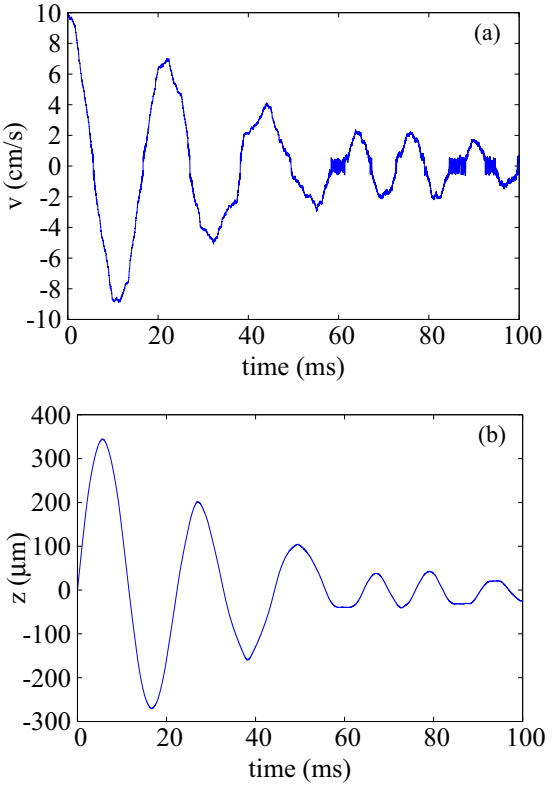

FIG. 9. (Color online) Example of a nanoparticle's motion in the field of the counterpropagating sequences of light pulses: (a) $v(t)$ and (b) $z(t)$. It is supposed that the mass of nanoparticle per every active atom is 30 000 Da. The parameters are $\tau = 1$ ps, $T = 10$ ns, $\vartheta = 0.1\pi$, $\gamma = 2\pi \times 10$ MHz, $\delta = 2\pi \times 5$ MHz, and $\lambda = 600$ nm. The nanoparticle starts at the center of the trap with initial velocity $v_0 = 10$ cm/s.

pieces. These pieces correspond to keeping the molecule in the state g_2, where the interaction of the molecule with the field is much weaker than in the state g_1. Between these pieces the velocity time dependence resembles one of the two-level atoms in the field of the counterpropagating pulse trains, shown in Fig. 3(a). The capture range of the trap for the parameters specified in Fig. 7 extends at least from $v = -12$ to 12 m/s.

The time dependences of the average coordinate $\bar{z} = \langle z \rangle$, average velocity $\bar{v} = \langle v \rangle$, $\Delta v = \sqrt{\langle v^2 \rangle - \langle v \rangle^2}$, and Δz for an ensemble of 400 molecules are depicted in Fig. 8. Approximately after 10 μs the ensemble of molecules with equal initial velocity becomes localized in the vicinity of the coordinate origin with $\Delta z = 112$ μm and $\Delta v = 12.2$ cm/s, which is slightly larger than 11.4 cm/s, corresponding to $T_{\min} = 168$ μK.

C. Potential for the nanoparticle light pulse trap

Let us suppose that a nanoparticle includes active atoms whose energetic levels almost are not perturbed by the interaction with neighboring atoms (for example, rare-earth atoms). We can estimate the behavior of the nanoparticle in the field of the counterpropagating pulses by analyzing the motion of the hypothetical two-level atom with mass equal to $M = M_{\rm np}/N_a$, where $M_{\rm np}$ is the mass of the nanoparticle and N_a is the number of active atoms. Figure 9 shows an example of a nanoparticle's motion in the field of the counterpropagating sequences of light pulses. The pulse's propagation direction is normal to the gravity acceleration. As in the case of a sodium atom, the nanoparticle oscillates around the coordinate origin, where the counterpropagating pulses collide. The amplitude of the oscillations decays in the case $\delta > 0$. Sometimes the nanoparticle oscillates in the vicinity of the field's nodes, which can be seen in Fig. 9 (for example, at -30.6, -30.9, -31.5, and -31.8 μm) jumping from one node to another neighboring node. The period of such an oscillation is $\sim$160 μs. The results of calculations show the strong potential for experimental realization of the trap for nanoparticles with included active atoms.

VIII. CONCLUSION

We simulated atomic and molecular motion (one particle and an ensemble of particles) in the field of weak counterpropagating light pulses and showed that these pulses form a light trap that, in addition to trapping the particles, cools them down to the Doppler temperature limit. We used the two-level model of the atom-field interaction to analyze atoms. The molecules in the trap were analyzed in the approximation of the three-level Λ-type model, which can be applicable for the molecules with almost diagonal Frank-Condon factor arrays. The parameter of the molecule-field interaction must eliminate the two-photon resonance condition. The velocity

capture range for atoms and molecules exceeds 10 m/s and the spatial capture range is about 100 μm.

We also discussed the applicability of the trap to confinement of nanoparticles, assuming that the nanoparticles include active atoms, i.e., atoms with transitions close to the carrier frequency of the pulses. The simulation result shows the strong potential for the realization of such a trap.

Recently, the frequency-comb-induced radiative force on cold rubidium atoms was investigated for single-pulse-train excitation and two-counterpropagating-pulse-train excitation [34]. The delay between counterpropagating pulses was close to 1 ns, which moves the point where the counterpropagating pulses collide far off the center of the trap. The experimental setup in [34] is suitable for the test of the trap based on counterpropagating laser pulses provided the parameters of the atom-field interaction (the time delay between pulses, the pulse area, and the frequency detuning) are properly chosen. As long as the atomic sample was a cloud of ^{87}Rb atoms trapped and cooled in the magneto-optical trap (MOT), the double trap, consisting of the MOT and the pulse trap, could be formed. Varying the pulse carrier frequency detuning from the transition frequency, one can see the change of the trapped cloud size in comparison with the no-pulse case and check if the trap based on the counterpropagating pulses is realized.

ACKNOWLEDGMENTS

This research was supported by the State goal-oriented scientific and engineering program "Nanotechnologies and Nanomaterials" of Ukraine (State goal-oriented scientific and engineering program "Nanotechnologies and Nanomaterials" is the name of scientific program supported by the government of Ukraine during 2010-2014) (Project No. 1.1.4.13/14-H25) and the State Fund for Fundamental Research of Ukraine (Project No. F53.2/001).

[1] S. Chu, Rev. Mod. Phys. **70**, 685 (1998).
[2] C. N. Cohen-Tannoudji, Rev. Mod. Phys. **70**, 707 (1998).
[3] W. D. Phillips, Rev. Mod. Phys. **70**, 721 (1998).
[4] P. Strohmeier, T. Kersebom, E. Kruger, H. Nolle, B. Steuter, J. Schmand, and J. Andra, Opt. Commun. **73**, 451 (1989).
[5] P. Strohmeier, A. Horn, T. Kersebom, and J. Schmand, Z. Phys. D **21**, 215 (1991).
[6] M. Watanabe, R. Ohmukai, U. Tanaka, K. Hayasaka, H. Imajo, and S. Urabe, J. Opt. Soc. Am. B **13**, 2377 (1996).
[7] K. Mølmer, Phys. Rev. Lett. **66**, 2301 (1991).
[8] D. Kielpinski, Phys. Rev. A **73**, 063407 (2006).
[9] E. Ilinova, M. Ahmad, and A. Derevianko, Phys. Rev. A **84**, 033421 (2011).
[10] D. Aumiler and T. Ban, Phys. Rev. A **85**, 063412 (2012).
[11] E. Ilinova and A. Derevianko, Phys. Rev. A **86**, 023417 (2012).
[12] T. G. M. Freegarde, J. Waltz, and W. Hänsch, Opt. Commun. **117**, 262 (1995).
[13] A. Goepfert, I. Bloch, D. Haubrich, F. Lison, R. Schütze, R. Wynands, and D. Meschede, Phys. Rev. A **56**, R3354(R) (1997).
[14] V. I. Romanenko and L. P. Yatsenko, J. Phys. B **44**, 115305 (2011).
[15] V. I. Balykin, JETP Lett. **81**, 209 (2005).
[16] D. N. Yanyshev, V. I. Balykin, Y. V. Vladimirova, and V. N. Zadkov, Phys. Rev. A **87**, 033411 (2013).
[17] V. I. Romanenko, A. V. Romanenko, Ye. G. Udovitskaya, and L. P. Yatsenko, Ukr. J. Phys. **58**, 438 (2013).
[18] V. I. Romanenko, A. V. Romanenko, Ye. G. Udovitskaya, and L. P. Yatsenko, J. Mod. Opt. **61**, 839 (2014).
[19] C. Mølmer, Y. Castin, and J. Dalibard, J. Opt. Soc. Am. B **10**, 524 (1993).
[20] H. J. Metcalf and P. van der Stratten, *Laser Cooling and Trapping* (Springer, New York, 1999).
[21] V. G. Minogin and V. S. Letokhov, *Laser Light Pressure on Atoms* (Gordon & Breach, New York, 1987).
[22] V. S. Voĭtsekhovich, M. V. Danileĭko, A. M. Negriĭko, V. I. Romanenko, and L. P. Yatsenko, Zh. Eksp. Teor. Fiz. **99**, 393 (1991) [Sov. Phys. JETP **72**, 219 (1991)].
[23] J. F. Barry, E. S. Shuman, E. B. Norrgard, and D. DeMille, Phys. Rev. Lett. **108**, 103002 (2012).
[24] M. D. Di Rosa, Eur. Phys. J. D **31**, 395 (2004).
[25] V. S. Voĭtsekhovich, M. V. Danileĭko, A. M. Negriĭko, V. I. Romanenko, and L. P. Yatsenko, JETP Lett. **59**, 408 (1994).
[26] B. W. Shore, *The Theory of Coherent Atomic Excitation* (Wiley, New York, 1990), Vol. 1.
[27] K. Bergmann, H. Theur, and B. W. Shore, Rev. Mod. Phys. **70**, 1003 (1998).
[28] N. V. Vitanov, T. Halfmann, B. W. Shore, and K. Bergmann, Annu. Rev. Phys. Chem. **52**, 763 (2001).
[29] V. I. Romanenko, Ukr. J. Phys. **51**, 1054 (2006).
[30] J. Steinbach, B. M. Garraway, and P. L. Knight, Phys. Rev. A **51**, 3302 (1995).
[31] C. S. Adams and E. Riis, Prog. Quantum Electron. **21**, 1 (1997).
[32] I. M. Sobol, *The Monte Carlo Method* (University of Chicago Press, Chicago, 1974).
[33] E. Ilinova and A. Derevianko, Phys. Rev. A **86**, 013423 (2012).
[34] G. Kregar, N. Šantić, D. Aumiler, H. Buljan, and T. Ban, Phys. Rev. A **89**, 053421 (2014).